



**Meteorological  
drivers of air quality  
extremes**

W. C. Porter et al.

This discussion paper is/has been under review for the journal Atmospheric Chemistry and Physics (ACP). Please refer to the corresponding final paper in ACP if available.

# Investigating the observed sensitivities of air quality extremes to meteorological drivers via quantile regression

W. C. Porter<sup>1</sup>, C. L. Heald<sup>1</sup>, D. Cooley<sup>2</sup>, and B. Russell<sup>2</sup>

<sup>1</sup>Massachusetts Institute of Technology, Cambridge, Massachusetts, USA

<sup>2</sup>Colorado State University, Fort Collins, Colorado, USA

Received: 23 March 2015 – Accepted: 15 April 2015 – Published: 19 May 2015

Correspondence to: W. C. Porter (wporter@mit.edu)

Published by Copernicus Publications on behalf of the European Geosciences Union.

Title Page

Abstract

Introduction

Conclusions

References

Tables

Figures



Back

Close

Full Screen / Esc

Printer-friendly Version

Interactive Discussion



## Abstract

Air pollution variability is strongly dependent on meteorology. However, quantifying the impacts of changes in regional climatology on pollution extremes can be difficult due to the many non-linear and competing meteorological influences on the production, transport, and removal of pollutant species. Furthermore, observed pollutant levels at many sites show sensitivities at the extremes that differ from those of the overall mean, indicating relationships that would be poorly characterized by simple linear regressions. To address this challenge, we apply quantile regression to observed daily ozone ( $O_3$ ) and fine particulate matter ( $PM_{2.5}$ ) levels and reanalysis meteorological fields in the United States over the past decade to specifically identify the meteorological sensitivities of higher pollutant levels. From an initial set of over 1700 possible meteorological indicators (including 28 meteorological variables with 63 different temporal options) we generate reduced sets of  $O_3$  and  $PM_{2.5}$  indicators for both summer and winter months, analyzing pollutant sensitivities to each for response quantiles ranging from 2–98 %. Primary drivers of high-quantile  $O_3$  levels include temperature and relative humidity in the summer, while winter  $O_3$  levels are most commonly associated with incoming radiation flux. Drivers of summer  $PM_{2.5}$  include temperature, wind speed, and tropospheric stability at many locations, while stability, humidity, and planetary boundary layer height are the key drivers most frequently associated with winter  $PM_{2.5}$ . We find key differences in driver sensitivities across regions and quantiles. For example, we find nationally averaged sensitivities of 95th percentile summer  $O_3$  to changes in maximum daily temperature of approximately  $0.9 \text{ ppb } ^\circ\text{C}^{-1}$ , while the sensitivity of 50th percentile summer  $O_3$  (the annual median) is only  $0.6 \text{ ppb } ^\circ\text{C}^{-1}$ . This gap points to differing sensitivities within various percentiles of the pollutant distribution, highlighting the need for statistical tools capable of identifying meteorological impacts across the entire response spectrum.

## Meteorological drivers of air quality extremes

W. C. Porter et al.

Title Page

Abstract

Introduction

Conclusions

References

Tables

Figures



Back

Close

Full Screen / Esc

Printer-friendly Version

Interactive Discussion





projections, as well as sound pollution control strategies. However, while straightforward sensitivity analyses using long-term averages and simple linear regressions provide valuable information on mean pollutant behavior, they are insufficient for analyses of extreme behaviors. Drivers and sensitivities characteristic of average pollutant responses will not necessarily be reflected throughout the entire pollutant distribution. To evaluate these relationships statistically, alternative methodologies must be used.

Previous studies examining the impact of meteorology on pollution levels have addressed the problem using a variety of tools. Modeling sensitivity studies offer a direct means of comparing the impacts of large-scale scenarios or individually adjusted parameters, allowing for a degree of comparison and replication that is impossible using only observations (e.g. Hogrefe et al., 2004; Mickley et al., 2004; Murazaki and Hess, 2006; Steiner et al., 2006; Heald et al., 2008). From such output, pollutant levels under multiple conditions or scenarios can be evaluated more or less in the same way that observed levels are, including the examination of global burdens, regional patterns, or even local exceedance frequencies as a function of meteorological changes. However, while these tools are powerful, it can be difficult to verify and understand projected changes due to the high degree of complexity of these models. On the other hand, observation-based examinations (e.g. Bloomer et al., 2009; Rasmussen et al., 2012) are tied closely to the actual underlying physical processes producing changes in pollutant levels, but are naturally limited in terms of identifying and quantifying the impacts of individual drivers – it is difficult to separate the impacts of different meteorological factors without the benefit of multiple sensitivity comparisons afforded by models.

Ordinary least-squares (OLS) regressions are effective tools for identifying trends and sensitivities in the distribution of pollution levels as a whole, especially for well-behaved data showing uniform sensitivities. Previous studies have analyzed the impacts of changes in specific meteorological conditions on O<sub>3</sub> and PM<sub>2.5</sub> levels (e.g. Brasseur et al., 2006; Liao et al., 2006), finding connections between weather patterns and mean pollutant response. In particular, the sensitivity of surface O<sub>3</sub> levels to changes in climate – the so-called “climate change penalty” (Wu et al., 2008) – has

## Meteorological drivers of air quality extremes

W. C. Porter et al.

[Title Page](#)[Abstract](#)[Introduction](#)[Conclusions](#)[References](#)[Tables](#)[Figures](#)[Back](#)[Close](#)[Full Screen / Esc](#)[Printer-friendly Version](#)[Interactive Discussion](#)

5 been examined in multiple studies worldwide (e.g. Bloomer et al., 2009), but previous examinations of individual meteorological sensitivities have typically produced single, monivariate estimates for changes in  $O_3$  given changes in each driver (e.g. temperature). However, when the variability of a given response is itself a function of the independent variable (i.e. the distribution “fans out”), the information provided by such regressions is less valuable for describing the specific response across the distribution – especially the extremes (Fig. 1a). If the sensitivities of  $O_3$  extremes to temperature tend to be higher than those of median to low  $O_3$  days (as is the case at many polluted locations), a single sensitivity value would underestimate the increase in extreme  $O_3$  event frequencies and magnitudes, given rising temperatures. This kind of behavior can be more effectively characterized through the use of more advanced statistical tools, such as quantile regression (Koenker and Bassett Jr., 1978). By linearizing and weighting the cost function of OLS regression, quantile regression (QR) allows for the quantification of sensitivity across the entire distribution of response levels, with the higher quantile regression slopes showing the behavior of the response variable’s high values and the lower quantiles showing the behavior of the low values as a function of any given indicator variable (Fig. 1b). Here, we apply multivariate QR to an analysis of meteorological drivers of  $O_3$  and  $PM_{2.5}$ , with the goal of identifying the drivers most responsible for changes in peak pollutant levels throughout the United States, and how these differ from the median response. Such a statistical examination of historical observations can provide a valuable reference point for the evaluation of model-predicted extremes, as well as a platform for short-term pollutant projections.

## 2 Methodology

### 2.1 Inputs

25 We use  $O_3$  and  $PM_{2.5}$  measurements from the US Environmental Protection Agency’s (EPA) Air Quality System (AQS) network, including daily peak 8 h average measure-

## Meteorological drivers of air quality extremes

W. C. Porter et al.

Title Page

Abstract

Introduction

Conclusions

References

Tables

Figures



Back

Close

Full Screen / Esc

Printer-friendly Version

Interactive Discussion





## Meteorological drivers of air quality extremes

W. C. Porter et al.

Title Page

Abstract

Introduction

Conclusions

References

Tables

Figures



Back

Close

Full Screen / Esc

Printer-friendly Version

Interactive Discussion



5 tant concentrations at many sites around the world, especially in coastal regions where diurnal wind patterns are prone to recirculation (Alper-Siman Tov et al., 1997; St. John and Chameides, 1997; Yimin and Lyons, 2003; Zhao et al., 2009). When air masses are returned to a site with ongoing emissions, the buildup of precursor concentrations may generate exceptionally high pollutant levels. To measure this effect we calculate a daily Recirculation Potential Index (RPI) from surface wind speeds, indicating the ratio between the summed vector and scalar magnitudes of 3 hourly wind speeds over the previous 24 h (Levy et al., 2009). A high RPI (close to 1) indicates that, regardless of average wind-velocity magnitudes, the total displacement of air over the previous 24 h was low, potentially leading to a pollutant buildup. Meanwhile, a very low RPI (close to 0) indicates steady, consistent wind, advecting air masses away from a location.

10 Stagnation, or the relative stability of tropospheric air masses, is another meteorological phenomenon previously cited as a driver of pollutant extremes (Banta et al., 1998; Jacob and Winner, 2009; Valente et al., 1998). While some of the raw meteorological fields (e.g. wind speed and precipitation) are already themselves good indicators of local stagnation, Lower Tropospheric Stability (LTS), the difference between surface and 700 hPa potential temperatures, is also calculated as a reflection of temperature inversion strength in the lower troposphere (Klein and Hartmann, 1993). Temperature inversions, in which the daytime pattern of air being warmer near the Earth's surface is reversed, generally lead to stable, stagnant conditions well suited for the buildup of pollutants such as  $O_3$  and  $PM_{2.5}$ . This phenomenon can be particularly pronounced in areas with geographical barriers to horizontal transport, such as the basins of Los Angeles and Salt Lake City (Langford et al., 2010; Pope, 1991).

25 From the selected set of raw and derived NARR meteorological fields (Table 1), we generate a range of temporal variables for each individual meteorological variable, including extrema and means for each 24 h day, as well as for 8 h daytime and previous 8 h nighttime ranges. To include possible long-term impacts of these meteorological variables, each of the 9 daily values are then extended into 3 and 6 day maxima, min-

ima, and means, as well as a 1 day delta variable to show 24 h change, resulting in 63 total temporal options for each listed meteorological variable.

### 2.3 Fire proximity metric

Biomass burning emissions can impact pollutant concentrations (e.g. Streets et al., 2003) with indirect correlations to daily meteorological variability, making it a potentially confounding factor when performing analyses using meteorological variables alone. To help examine and quantify the likely impact of fires on observed pollutant levels we create a simple fire metric to represent the spatial and temporal proximity of each site to satellite-observed burn locations. Using output from the Moderate Resolution Imaging Spectroradiometer (MODIS) Global Monthly Fire Location Product (Giglio et al., 2003; Justice et al., 2002) we estimate the total fire proximity impact for each site by applying spatial and temporal decays to burn detection confidence values, and summing these values across all detected pixels through the equation

$$F = \log \left( \sum_i \frac{1}{r} \frac{1}{2^t} \text{conf} \right). \quad (1)$$

Here, the fire proximity index  $F$  is a function of the distance ( $r$ ) and number of elapsed days ( $t$ , ranging from 0 to 6) separating a station from a MODIS-detected burn pixel with a given confidence value (conf), summed over all nearby burn pixels  $i$ . The resulting proximity metric does not take transport, precipitation, or any other meteorological variables into account, simply producing higher values for stations near burning (or recently burned) locations. A comprehensive treatment of biomass burning emissions and transport requires accurate information on many complex factors, including fuel type, burn intensity, and smoke injection heights (Val Martin et al., 2010; Wiedinmyer et al., 2011), and fully representing these factors to generate a robust estimate for the influence of fire emissions goes well beyond the scope of this work. However, considering both the stochastic nature of large fire events and the importance of biomass

## Meteorological drivers of air quality extremes

W. C. Porter et al.

Title Page

Abstract

Introduction

Conclusions

References

Tables

Figures



Back

Close

Full Screen / Esc

Printer-friendly Version

Interactive Discussion







5 tor candidates, using both time and the recently added variable as fixed covariates. We repeat this cycle until no temporal candidates remain for the current meteorological variable, after which the temporal variable selection starts anew with the next meteorological parameter. Once temporal variable options have been filtered down for each individual meteorological driver through this selection process we gather all selected variables together and apply the same selection process to the full set of approximately 300 candidates, finally arriving at trimmed down set of less than 20 meteorological indicators for each pollutant species and season (Table 2, top). The selection process is somewhat sensitive to the percentile used for the regression, as evidenced by the different variables selected using the 50th percentile rather than the 90th (Table 2, below). While most high-ranked meteorological variables show up using both selection processes, there are noticeable differences, especially in the temporal options chosen.

10 Through this routine, variables can stand out for selection by being either moderately important at many sites, or by being very important at fewer sites. By adjusting the threshold parameter for variable selection, the scope of variable inclusion can be tuned to a certain extent. In this work we identify and compare both a concise “Core” set of indicators (summed inverse rank threshold of at least 2) and a “Full” set of indicators (relaxed summed inverse rank threshold of at least 1).

## 2.5 Quantile regression

20 The final sets of indicator variables represent those drivers most broadly responsible for variability in high pollutant levels due to meteorological factors at the 100 chosen test sites. Using these selected meteorological variables we next perform multivariate quantile regression to identify sensitivities for percentiles from 2 to 98 % at each station in the full set of AQS sites. From these regressions we collect Summer (JJA) and Winter (DJF) quantile sensitivities of  $O_3$  and  $PM_{2.5}$  to each meteorological variable for each AQS station.

### Meteorological drivers of air quality extremes

W. C. Porter et al.

Title Page

Abstract

Introduction

Conclusions

References

Tables

Figures



Back

Close

Full Screen / Esc

Printer-friendly Version

Interactive Discussion



### 3 Results

To assess relative driver importance across the United States we normalize quantile sensitivities to standard deviations of pollutant and indicator fluctuations and rank them in relation to each other at each site. Top-ranking covariates for any given station, then, are those whose variabilities (in normalized units of standard deviations) are most responsible for variability in the observed pollutant. Figures 3 and 5 show each variable's frequency of appearing as the first or second most important indicator by this metric, with similar variables grouped together into columns. We compare the drivers of the 95th and 50th percentile of pollutant concentrations, finding similar, though not identical, frequencies between top performers for the two quantiles.

#### 3.1 O<sub>3</sub> drivers – summer

In the summertime, drivers of high-percentile O<sub>3</sub> are dominated by a positive correlation with temperature at most sites (Fig. 3a, top), consistent with previous modeling sensitivity conclusions (Jacob and Winner, 2009). Altogether, 49 % of the analyzed sites show maximum daily surface air temperature as the meteorological variable with the greatest normalized slope relative to observed maximum 8 h average O<sub>3</sub> concentrations, and it is within the top five most influential variables at 79 % of all sites. Underlying reasons for the dominance of temperature as a driver of observed O<sub>3</sub> include a positive correlation with biogenic emissions of isoprene (a potential precursor of O<sub>3</sub>), a negative correlation with the lifetime of peroxyacetylnitrate (PAN, an important reservoir species for NO<sub>x</sub> and HO<sub>x</sub> radicals), and an associated correlation between higher temperatures and bright, stagnant conditions (Jacob and Winner, 2009).

While maximum daily surface temperature stands out as the covariate with the highest normalized impact on daily summer O<sub>3</sub> levels, many other variables also play important roles, especially in the south and southeast regions (Fig. 3a, bottom). Water vapor generally reduces O<sub>3</sub> levels under pristine conditions, removing dissociated excited oxygen atoms and producing the hydroxyl radical (OH). Under polluted conditions

Title Page

Abstract

Introduction

Conclusions

References

Tables

Figures



Back

Close

Full Screen / Esc

Printer-friendly Version

Interactive Discussion



5 this negative effect competes with increased  $O_3$  production as a result of OH reacting with carbon monoxide (CO) or volatile organic compounds (VOCs),  $O_3$  precursors common to highly polluted environments. These two effects combine to produce generally weak correlations between humidity and  $O_3$  in model perturbation studies (Jacob and Winner, 2009). In this work, however, relative humidity (RH) has a strong negative relationship with  $O_3$  in many locations, particularly in the south, consistent with previous analyses of observed sensitivities (e.g. Camalier et al., 2007). An inverse correlation with temperature and a positive correlation with cloudy, unstable conditions may explain the stronger associations found in the observations relative to those of model perturbation studies. Stability, in the form of turbulent kinetic energy (TKE) is also a strong performer at many sites, though less so for the 95th percentile than for the 50th. Finally, while fire proximity stands out at relatively few stations as a dominant driver of median  $O_3$  levels (50th percentile), it appears to be important at far more sites when examining higher  $O_3$  levels (95th percentile).

10 While the top driver frequencies shown in Fig. 3a can help identify dominant meteorological drivers overall, they do not indicate spatial distributions or sensitivity magnitudes. The bottom panel of Figs. 3a and 4 address these aspects of selected top drivers, showing where each tends to drive pollutant variability, as well as how the sensitivity magnitudes are distributed overall. Spatially, the temperature sensitivity of 95th percentile  $O_3$  levels appears to be most directly associated with coastal areas, though the strong negative relationship between relative humidity and  $O_3$  in the south likely includes temperature effects (Fig. 3, bottom). In general, the sensitivities of  $O_3$  to changes in temperature are greater for higher  $O_3$  quantiles, as shown by the increasing and flattening distributions for 95th quantile regression sensitivities compared to 50th and 5th quantile values (Fig. 4, upper left). In fact, quantile regression coefficients for the 95th percentiles averaged  $0.9 \text{ ppb } ^\circ\text{C}^{-1}$ , 50 % greater than mean 50th percentile sensitivities. This difference again highlights the importance of temperature in determining extreme  $O_3$  events, since increased temperatures could be expected to positively affect the magnitudes of high  $O_3$  days even more than would be expected

## Meteorological drivers of air quality extremes

W. C. Porter et al.

Title Page

Abstract

Introduction

Conclusions

References

Tables

Figures



Back

Close

Full Screen / Esc

Printer-friendly Version

Interactive Discussion



based on average days. By comparison, downward shortwave radiation flux also shows up as a positive driver of high O<sub>3</sub> levels, but displays much more consistent sensitivities across O<sub>3</sub> quantiles (Fig. 4, upper right).

### 3.2 O<sub>3</sub> drivers – winter

O<sub>3</sub> levels are generally lower at all percentiles during the winter months compared to the summer months, with 95th percentile O<sub>3</sub> levels almost halved at some sites. As seen in Fig. 3b, temperature is almost completely absent from the top ranks of O<sub>3</sub> indicators during the winter. Instead, variables related to incoming radiation flux are most important at many sites, especially for 95th percentile O<sub>3</sub> levels. This indicates the relative importance of consistently clear skies for O<sub>3</sub> production during the coldest months, a relationship that appears consistently across quantiles and regions (Fig. 3b, bottom). Among the incoming radiation metrics, the 6 day maximum of daily mean shortwave radiation flux showed up as a top driver most often, with consistently positive correlations evenly distributed spatially (Fig. 4, lower left). Sensitivities are slightly greater, on average, for higher quantiles, and stand out as particularly strong at stations in Wyoming, an area previously highlighted for its dangerously high winter O<sub>3</sub> levels (e.g. Schnell et al., 2009). As with summer O<sub>3</sub>, DSWRF again has a generally positive influence on winter O<sub>3</sub>, with some increase in sensitivity at higher quantiles (Fig. 4, lower right). HPBL, wind, and specific humidity show up as top drivers at many sites as well, but more so for median quantile regressions than for 95th regressions, while fire proximity becomes increasingly important at the higher quantiles.

### 3.3 PM<sub>2.5</sub> drivers – summer

Figure 5a shows that mean daily temperature is also a key player in predicting summertime PM<sub>2.5</sub>, with greater sensitivities at the highest concentration percentiles. While the previously discussed sensitivities of O<sub>3</sub> to temperature shown in Fig. 4 are greatest along both the Northeast coast and Southern California, PM<sub>2.5</sub> sensitivities to tem-

## Meteorological drivers of air quality extremes

W. C. Porter et al.

Title Page

Abstract

Introduction

Conclusions

References

Tables

Figures



Back

Close

Full Screen / Esc

Printer-friendly Version

Interactive Discussion



**Meteorological  
drivers of air quality  
extremes**

W. C. Porter et al.

Title Page

Abstract

Introduction

Conclusions

References

Tables

Figures



Back

Close

Full Screen / Esc

Printer-friendly Version

Interactive Discussion



perature peak entirely in the East. One possible reason for this spatial difference in  $PM_{2.5}$  temperature sensitivity is the regionality of  $PM_{2.5}$  speciation, especially in terms of competing sensitivities of nitrate and sulfate aerosol (Dawson et al., 2007). While concentrations of nitrate aerosol (and, to a lesser extent, organics) are generally reduced by higher temperatures due to increased gas phase partitioning, sulfate aerosol concentrations can increase at higher temperatures because of increased rates of oxidation. Sulfur emissions are far higher in the East than in the West, offering a likely explanation for the differing sensitivities of  $PM_{2.5}$  to temperature between the regions.

In addition to temperature, 95th percentile  $PM_{2.5}$  shows strong sensitivities to wind speeds and tropospheric stability at many sites, emphasizing the importance of transport and stagnancy for extreme  $PM_{2.5}$  events, particularly those in highly-polluted regions (Fig. 5a, bottom). 3 day averages wind speed stood out among drivers at many sites throughout the East and Midwest regions, and influences tended to be of higher magnitude for high-quantile  $PM_{2.5}$  levels than for medians or low quantiles (Fig. 6, upper right). Positive correlations for this metric may be associated with areas whose extremes were governed primarily by transport, rather than production. Also increasingly important for higher quantiles of fine particulate matter was fire proximity, with over twice as many sites including this metric in the top drivers for 95th percentile  $PM_{2.5}$  as for 50th percentile  $PM_{2.5}$ .

### 3.4 $PM_{2.5}$ drivers – winter

Unlike  $O_3$ , winter  $PM_{2.5}$  levels in the United States are often comparable to (or even greater than) those of the summer months at many sites (Fig. 2). Compared to other seasons and species, the dominant drivers of winter  $PM_{2.5}$  are more consistently distributed between a few key variables (Fig. 5b, top). Temperature is apparently less of a factor during cold months, rarely appearing among the top normalized indicators, and metrics related to stagnation stand out as important drivers of pollution events. Among meteorological drivers of increased winter  $PM_{2.5}$ , stability metrics (TKE and LTS), relative humidity, and planetary boundary layer height (HPBL), stood out as key variables



differ from the mean behavior. To put these changes in context, the overall mean sensitivity for each variable (in normalized units of standard deviations) is shown by color.

For summertime  $O_3$  and  $PM_{2.5}$ , temperature stands out as a driver that not only has a strong positive impact on concentrations (indicated by the bright red color), but also exhibits even stronger impacts on high percentile pollutant levels than on lower percentile levels at most stations. On the other hand, while HPBL also strongly impacts summertime  $O_3$ , the change in sensitivity between low and high quantiles is generally small, indicating a variable whose impact on  $O_3$  is relatively unchanging across pollutant percentiles. Besides temperature's impact on summer  $O_3$  and  $PM_{2.5}$ , the key drivers of winter  $PM_{2.5}$  stand out for having many changing quantile sensitivities. The sensitivity of  $PM_{2.5}$  to relative humidity, lower tropospheric stability, HPBL, and TKE are all greater for high  $PM_{2.5}$  quantiles than they are for low ones, highlighting the importance of characterizing the full pollutant response to meteorological drivers, especially for winter  $PM_{2.5}$ .

## 4.2 Overall predictive power of statistical models

The variables identified here were not selected based on their suitability for ordinary least squares regression, but they do show considerable skill at predicting pollutant levels using this methodology, explaining over half of the variability at most sites (Fig. 8). Predictive skill for summertime  $O_3$  is greatest in East, South, and Midwest (regions 2 through 6) and least in the Pacific Southwest and Mountains and Plains regions (regions 8 and 9). Winter  $O_3$   $R^2$  values are generally slightly lower than those of the summer months, especially in the Pacific Northwest and South Central regions, though this may be partly explained by reduced  $O_3$  variability overall in the winter months.

$PM_{2.5}$  shows a strong split between the relatively well-modeled Northeast and the less-accurately represented Midwest and Southwest. These results compare favorably to previous attempts to predict  $PM_{2.5}$  using meteorological indicators (Demuzere et al., 2009; Tai et al., 2010). Tai et al. (2010), for example, find multivariate linear regression capable of explaining less than 50% of  $PM_{2.5}$  variability in the Northeast United

States. Almost half of the stations in those same regions showed adjusted  $R^2$  values of greater than 60 % using our method, despite the indicators being chosen to optimize high quantile regressions rather than OLS regressions. Regional differences in meteorological predictive power in this work are also comparable to those of Tai et al., who found high  $R^2$  values in the Northeast and Pacific Northwest (regions 2, 3, and 5), and lower values in the South and Mountains and Plains regions (regions 6 and 8).

### 4.3 Pollutant variability and trend

It is apparent that relatively simple meteorological processes, chosen for their influence on high percentiles of  $O_3$  and  $PM_{2.5}$ , are also capable of explaining a large fraction of daily pollutant variability. There are a number of possible sources for the remaining variability, including day-to-day fluctuations in pollutant precursor emissions and highly localized meteorological patterns. While the nation-wide variable selection process of this study proved capable of identifying indicators that are broadly effective at predicting daily pollutant levels in many locations, specific features relevant to individual stations (e.g. direction and distance of upwind emission sources) may not be adequately represented by the globally selected variables. Variability in local emission sources themselves, either due to sporadic local events or differences in weekend vs. weekday emissions, may also play an important role at some sites. This analysis is also subject to uncertainties in the NARR product and the pollutant observations, as well as discrepancies between local station conditions and the grid-averaged NARR output.

Another important consideration in the analysis of these results is the nonstationarity of both pollutant concentrations and sensitivities. As a result of the implementation of widespread emissions controls, concentrations of  $O_3$  and  $PM_{2.5}$  have decreased dramatically in many of the most polluted areas in the United States. For stations with the most extensive record of summer  $O_3$  (at least 600 days of valid observations between 2004 and 2012), summertime maximum daily 8 h average  $O_3$  fell by  $0.2 \text{ ppb year}^{-1}$  on average. 95th percentile values at these same stations fell even more rapidly, by

Meteorological drivers of air quality extremes

W. C. Porter et al.

Title Page

Abstract Introduction

Conclusions References

Tables Figures

◀ ▶

◀ ▶

Back Close

Full Screen / Esc

Printer-friendly Version

Interactive Discussion





**Meteorological  
drivers of air quality  
extremes**

W. C. Porter et al.

Title Page

Abstract

Introduction

Conclusions

References

Tables

Figures



Back

Close

Full Screen / Esc

Printer-friendly Version

Interactive Discussion



We find that temperature is a dominant driver at most stations in the summer for both  $O_3$  and  $PM_{2.5}$ , with relative humidity, stability, and radiation flux also key drivers for  $O_3$ , and wind, stability, and rain often important for predicting high  $PM_{2.5}$  levels.  $O_3$  variability during winter months is determined largely by changes in incoming radiation, while winter  $PM_{2.5}$  extremes are most commonly affected by stagnation, humidity, and PBL height. We show substantial regional variation in these results, suggesting that while classes of drivers of extreme air quality are generally consistent, specific factors leading to air quality exceedances are local.

Climate change in coming decades is likely to induce a response in regional air pollution. The sensitivities of  $O_3$  and  $PM_{2.5}$  to changes in meteorological patterns are, in general, stronger for higher pollution percentiles, meaning that changes to certain drivers (most notably temperature, wind speed, PBL height, and tropospheric stability) are likely to affect the magnitude and frequencies of pollutant extremes more drastically than they affect more moderate pollution levels. This effect suggests that regional changes to climate could have more significant impacts on the frequencies of extreme  $O_3$  and  $PM_{2.5}$  events than would be suggested by bulk sensitivities from OLS regressions.

This analysis framework offers new ways to investigate both the observed and simulated air-quality responses to climate. Through quantile regression, the selection and ranking of key drivers of pollutant variability can be evaluated robustly, focusing not on the mean behavior of a heavy-tailed pollutant distribution, but rather the sensitivities closer to the tail itself. Furthermore, the comparison of observed sensitivities to those simulated by regional or global air quality models could identify key model biases relevant to the projection of future air quality, potentially providing insights on the underlying mechanistic reasons for those biases.

*Acknowledgements.* This work was supported by the EPA-STAR program. Although the research described in this article has been funded by the US EPA through grant/cooperative agreement (RD-83522801), it has not been subjected to the Agency's required peer and policy

review and therefore does not necessarily reflect the views of the Agency and no official endorsement should be inferred. The authors acknowledge Brian J. Reich for useful discussions.

## References

- Alper-Siman Tov, D., Peleg, M., Matveev, V., Mahrer, Y., Seter, I., and Luria, M.: Recirculation of polluted air masses over the East Mediterranean coast, *Atmos. Environ.*, 31, 1441–1448, doi:10.1016/S1352-2310(96)00321-4, 1997.
- Banta, R. M., Senff, C. J., White, A. B., Trainer, M., McNider, R. T., Valente, R. J., Mayor, S. D., Alvarez, R. J., Hardesty, R. M., Parrish, D., and Fehsenfeld, F. C.: Daytime buildup and nighttime transport of urban ozone in the boundary layer during a stagnation episode, *J. Geophys. Res.*, 103, 22519–22544, doi:10.1029/98JD01020, 1998.
- Bell, M. L., Dominici, F., and Samet, J. M.: A meta-analysis of time-series studies of ozone and mortality with comparison to the national morbidity, mortality, and air pollution study, *Epidemiology*, 16, 436–445, doi:10.1097/01.ede.0000165817.40152.85, 2005.
- Bloomer, B. J., Stehr, J. W., Piety, C. A., Salawitch, R. J., and Dickerson, R. R.: Observed relationships of ozone air pollution with temperature and emissions, *Geophys. Res. Lett.*, 36, L09803, doi:10.1029/2009GL037308, 2009.
- Brasseur, G. P., Schultz, M., Granier, C., Saunois, M., Diehl, T., Botzet, M., Roeckner, E., and Walters, S.: Impact of climate change on the future chemical composition of the global troposphere, *J. Climate*, 19, 3932–3951, 2006.
- Burnham, K. P. and Anderson, D. R.: Multimodel inference understanding AIC and BIC in model selection, *Sociol. Method. Res.*, 33, 261–304, doi:10.1177/0049124104268644, 2004.
- Camalier, L., Cox, W., and Dolwick, P.: The effects of meteorology on ozone in urban areas and their use in assessing ozone trends, *Atmos. Environ.*, 41, 7127–7137, doi:10.1016/j.atmosenv.2007.04.061, 2007.
- Dawson, J. P., Adams, P. J., and Pandis, S. N.: Sensitivity of PM<sub>2.5</sub> to climate in the Eastern US: a modeling case study, *Atmos. Chem. Phys.*, 7, 4295–4309, doi:10.5194/acp-7-4295-2007, 2007.
- Demuzere, M., Trigo, R. M., Vila-Guerau de Arellano, J., and van Lipzig, N. P. M.: The impact of weather and atmospheric circulation on O<sub>3</sub> and PM<sub>10</sub> levels at a rural mid-latitude site, *Atmos. Chem. Phys.*, 9, 2695–2714, doi:10.5194/acp-9-2695-2009, 2009.

## Meteorological drivers of air quality extremes

W. C. Porter et al.

Title Page

Abstract

Introduction

Conclusions

References

Tables

Figures



Back

Close

Full Screen / Esc

Printer-friendly Version

Interactive Discussion



## Meteorological drivers of air quality extremes

W. C. Porter et al.

Title Page

Abstract

Introduction

Conclusions

References

Tables

Figures



Back

Close

Full Screen / Esc

Printer-friendly Version

Interactive Discussion



Dockery, D. W., Pope, C. A., Xu, X., Spengler, J. D., Ware, J. H., Fay, M. E., Ferris, B. G., and Speizer, F. E.: An association between air pollution and mortality in six US cities, *New Engl. J. Med.*, 329, 1753–1759, doi:10.1056/NEJM199312093292401, 1993.

Geraci, M. and Bottai, M.: Quantile regression for longitudinal data using the asymmetric Laplace distribution, *Biostatistics*, 8, 140–154, doi:10.1093/biostatistics/kxj039, 2007.

Giglio, L., Descloitres, J., Justice, C. O., and Kaufman, Y. J.: An enhanced contextual fire detection algorithm for MODIS, *Remote Sens. Environ.*, 87, 273–282, doi:10.1016/S0034-4257(03)00184-6, 2003.

Heald, C. L., Henze, D. K., Horowitz, L. W., Feddema, J., Lamarque, J.-F., Guenther, A., Hess, P. G., Vitt, F., Seinfeld, J. H., Goldstein, A. H., and Fung, I.: Predicted change in global secondary organic aerosol concentrations in response to future climate, emissions, and land use change, *J. Geophys. Res.*, 113, 1–16, doi:10.1029/2007JD009092, 2008.

Hogrefe, C., Lynn, B., Civerolo, K., Ku, J.-Y., Rosenthal, J., Rosenzweig, C., Goldberg, R., Gaffin, S., Knowlton, K., and Kinney, P. L.: Simulating changes in regional air pollution over the eastern United States due to changes in global and regional climate and emissions, *J. Geophys. Res.*, 109, D22301, doi:10.1029/2004JD004690, 2004.

Jacob, D. J. and Winner, D. A.: Effect of climate change on air quality, *Atmos. Environ.*, 43, 51–63, doi:10.1016/j.atmosenv.2008.09.051, 2009.

Jerrett, M., Burnett, R. T., Pope, C. A., Ito, K., Thurston, G., Krewski, D., Shi, Y., Calle, E., and Thun, M.: Long-term ozone exposure and mortality, *New Engl. J. Med.*, 360, 1085–1095, doi:10.1056/NEJMoa0803894, 2009.

Justice, C. O., Giglio, L., Korontzi, S., Owens, J., Morisette, J. T., Roy, D., Descloitres, J., Al-leaume, S., Petticolin, F., and Kaufman, Y.: The MODIS fire products, *Remote Sens. Environ.*, 83, 244–262, doi:10.1016/S0034-4257(02)00076-7, 2002.

Klein, S. A. and Hartmann, D. L.: The seasonal cycle of low stratiform clouds, *J. Climate*, 6, 1587–1606, doi:10.1175/1520-0442(1993)006<1587:TSCOLS>2.0.CO;2, 1993.

Koenker, R. and Bassett Jr., G.: Regression quantiles, *Econometrica*, 46, 33–50, 1978.

Krewski, D., Jerrett, M., Burnett, R. T., Ma, R., Hughes, E., Shi, Y., Turner, M. C., Pope, C. A., Thurston, G., Calle, E. E., Thun, M. J., Beckerman, B., DeLuca, P., Finkelstein, N., Ito, K., Moore, D. K., Newbold, K. B., Ramsay, T., Ross, Z., Shin, H., and Tempalski, B.: Extended follow-up and spatial analysis of the American Cancer Society study linking particulate air pollution and mortality, *Res. Rep. Health Eff. Inst.*, 140, 5–114, 2009.

## Meteorological drivers of air quality extremes

W. C. Porter et al.

Title Page

Abstract

Introduction

Conclusions

References

Tables

Figures



Back

Close

Full Screen / Esc

Printer-friendly Version

Interactive Discussion



Langford, A. O., Senff, C. J., Alvarez, R. J., Banta, R. M., and Hardesty, R. M.: Long-range transport of ozone from the Los Angeles basin: a case study, *Geophys. Res. Lett.*, 37, L06807, doi:10.1029/2010GL042507, 2010.

Lee, E. R., Noh, H., and Park, B. U.: Model selection via Bayesian information criterion for quantile regression models, *J. Am. Stat. Assoc.*, 109, 216–229, doi:10.1080/01621459.2013.836975, 2014.

Levy, I., Mahrer, Y., and Dayan, U.: Coastal and synoptic recirculation affecting air pollutants dispersion: a numerical study, *Atmos. Environ.*, 43, 1991–1999, doi:10.1016/j.atmosenv.2009.01.017, 2009.

Liao, H., Chen, W.-T., and Seinfeld, J. H.: Role of climate change in global predictions of future tropospheric ozone and aerosols, *J. Geophys. Res.*, 111, D12304, doi:10.1029/2005JD006852, 2006.

Val Martin, M., Logan, J. A., Kahn, R. A., Leung, F.-Y., Nelson, D. L., and Diner, D. J.: Smoke injection heights from fires in North America: analysis of 5 years of satellite observations, *Atmos. Chem. Phys.*, 10, 1491–1510, doi:10.5194/acp-10-1491-2010, 2010.

Mesinger, F., DiMego, G., Kalnay, E., Mitchell, K., Shafran, P. C., Ebisuzaki, W., Jović, D., Woollen, J., Rogers, E., Berbery, E. H., Ek, M. B., Yun Fan, Grumbine, R., Higgins, W., Hong Li, Ying Lin, Manikin, G., Parrish, D., and Wei Shi: North American regional reanalysis, *B. Am. Meteorol. Soc.*, 87, 343–360, doi:10.1175/BAMS-87-3-343, 2006.

Mickley, L. J., Jacob, D. J., Field, B. D., and Rind, D.: Effects of future climate change on regional air pollution episodes in the United States, *Geophys. Res. Lett.*, 31, L24103, doi:10.1029/2004GL021216, 2004.

Murazaki, K. and Hess, P.: How does climate change contribute to surface ozone change over the United States?, *J. Geophys. Res.*, 111, D05301, doi:10.1029/2005JD005873, 2006.

Pope 3rd, C. A.: respiratory hospital admissions associated with PM<sub>10</sub> pollution in Utah, Salt Lake, and Cache Valleys, *Arch. Environ. Health*, 46, 90–97, 1991.

Pope III, C. A., Ezzati, M., and Dockery, D. W.: Fine-particulate air pollution and life expectancy in the United States, *New Engl. J. Med.*, 360, 376–386, 2009.

Rasmussen, D. J., Fiore, A. M., Naik, V., Horowitz, L. W., McGinnis, S. J., and Schultz, M. G.: Surface ozone–temperature relationships in the eastern US: a monthly climatology for evaluating chemistry–climate models, *Atmos. Environ.*, 47, 142–153, doi:10.1016/j.atmosenv.2011.11.021, 2012.

## Meteorological drivers of air quality extremes

W. C. Porter et al.

Title Page

Abstract

Introduction

Conclusions

References

Tables

Figures



Back

Close

Full Screen / Esc

Printer-friendly Version

Interactive Discussion



- Schnell, R. C., Oltmans, S. J., Neely, R. R., Endres, M. S., Molenaar, J. V., and White, A. B.: Rapid photochemical production of ozone at high concentrations in a rural site during winter, *Nat. Geosci.*, 2, 120–122, doi:10.1038/ngeo415, 2009.
- Schwarz, G.: Estimating the dimension of a model, *Ann. Stat.*, 6, 461–464, doi:10.1214/aos/1176344136, 1978.
- St. John, J. C. and Chameides, W. L.: Climatology of ozone exceedences in the atlanta metropolitan area: 1-hour vs. 8-hour standard and the role of plume recirculation air pollution episodes, *Environ. Sci. Technol.*, 31, 2797–2804, doi:10.1021/es961068a, 1997.
- Steiner, A. L., Tonse, S., Cohen, R. C., Goldstein, A. H., and Harley, R. A.: Influence of future climate and emissions on regional air quality in California, *J. Geophys. Res.*, 111, D18303, doi:10.1029/2005JD006935, 2006.
- Streets, D. G., Bond, T. C., Carmichael, G. R., Fernandes, S. D., Fu, Q., He, D., Klimont, Z., Nelson, S. M., Tsai, N. Y., Wang, M. Q., Woo, J.-H., and Yarber, K. F.: An inventory of gaseous and primary aerosol emissions in Asia in the year 2000, *J. Geophys. Res.*, 108, 8809, doi:10.1029/2002JD003093, 2003.
- Tai, A. P. K., Mickley, L. J., and Jacob, D. J.: Correlations between fine particulate matter (PM<sub>2.5</sub>) and meteorological variables in the United States: implications for the sensitivity of PM<sub>2.5</sub> to climate change, *Atmos. Environ.*, 44, 3976–3984, doi:10.1016/j.atmosenv.2010.06.060, 2010.
- Valente, R. J., Imhoff, R. E., Tanner, R. L., Meagher, J. F., Daum, P. H., Hardesty, R. M., Banta, R. M., Alvarez, R. J., McNider, R. T., and Gillani, N. V.: Ozone production during an urban air stagnation episode over Nashville, Tennessee, *J. Geophys. Res.*, 103, 22555–22568, doi:10.1029/98JD01641, 1998.
- Wiedinmyer, C., Akagi, S. K., Yokelson, R. J., Emmons, L. K., Al-Saadi, J. A., Orlando, J. J., and Soja, A. J.: The Fire INventory from NCAR (FINN): a high resolution global model to estimate the emissions from open burning, *Geosci. Model Dev.*, 4, 625–641, doi:10.5194/gmd-4-625-2011, 2011.
- Wu, S., Mickley, L. J., Leibensperger, E. M., Jacob, D. J., Rind, D., and Streets, D. G.: Effects of 2000–2050 global change on ozone air quality in the United States, *J. Geophys. Res.*, 113, D06302, doi:10.1029/2007JD008917, 2008.
- Yang, Y.: Can the strengths of AIC and BIC be shared? A conflict between model identification and regression estimation, *Biometrika*, 92, 937–950, doi:10.1093/biomet/92.4.937, 2005.

Yimin, M. and Lyons, T. J.: Recirculation of coastal urban air pollution under a synoptic scale thermal trough in Perth, Western Australia, *Atmos. Environ.*, 37, 443–454, 2003.  
Zhao, C., Wang, Y., and Zeng, T.: East China plains: a “basin” of ozone pollution, *Environ. Sci. Technol.*, 43, 1911–1915, doi:10.1021/es8027764, 2009.

**Meteorological drivers of air quality extremes**

W. C. Porter et al.

Title Page

Abstract

Introduction

Conclusions

References

Tables

Figures



Back

Close

Full Screen / Esc

Printer-friendly Version

Interactive Discussion





**Meteorological drivers of air quality extremes**

W. C. Porter et al.

**Table 2.** Selected drivers for O<sub>3</sub> and PM<sub>2.5</sub> using 90th percentile (above) and 50th percentile (below) quantile regressions. “Core” drivers (in bold) were selected using a minimum threshold for summed inverted ranks of at least 2, with remaining drivers added by rerunning the selection procedure including all Core variables and a relaxed selection threshold of 1.

| Selected via 90th Percentile QR |                               |                               |                                |
|---------------------------------|-------------------------------|-------------------------------|--------------------------------|
| Summer O <sub>3</sub>           | Summer PM <sub>2.5</sub>      | Winter O <sub>3</sub>         | Winter PM <sub>2.5</sub>       |
| rhum.2m_mean                    | air.2m_max                    | dsrwrf_mean.6daymax           | hpbl_mean                      |
| vwnddir.10m_mean                | vwnddir.10m_mean              | wspd.10m_mean                 | vwnddir.10m_mean               |
| air.2m_max                      | lftx4_daymin                  | vwnddir.10m_mean              | tke.hl1_9x9_daymax.3daymean    |
| crain_9x9_daymean               | uwnddir.10m_mean.3daymean     | rhum.2m_min                   | wspd.10m_nightmax              |
| fire                            | wspd.10m_max.3daymean         | fire                          | rhum.2m_mean                   |
| uwnddir.10m_mean                | air.sfc_9x9_nightmin.6daymean | rpi_max                       | shum.2m_daymax.6daymin         |
| air.sfc_9x9_min.6daymin         | fire                          | hpbl_daymax                   | crain_9x9_nightmean            |
| pres.sfc_daymax                 | crain_9x9_max.6daymean        | air.sfc_9x9_nightmin.6daymean | lts_min.3daymin                |
| tke.hl1_9x9_max                 | vwnddir.10m_daymean.6daymean  | dlwrf_daymax.6daymin          | uwnddir.10m_mean.3daymean      |
| dsrwrf_daymin.3daymean          | apcp_nightmax                 | crain_9x9_max                 | dsrwrf_max.3daymean            |
| hpbl_max                        | rpi_nightmin                  | uwnddir.10m_daymean           | lftx4_nightmin.6daymin         |
| tcdc_9x9_mean                   | vvel.hl1_nightmax.6daymax     | tcdc_9x9_mean                 | wspd.500_min                   |
| dsrwrf_min.6daymin              | hpbl_nightmax.6daymax         | lts_nightmax.3daymin          | tke.hl1_9x9_max.6daymin        |
| vwnd.500_daymax.3daymean        | rpi_nightmax.6daymin          | lftx4_min.diff                | vwnd.500_max.diff              |
| shum.2m_max.diff                | tcdc_9x9_max.6daymax          | lctdc_9x9_nightmin.6daymax    | tcdc_9x9_max.diff              |
| wspd.10m_daymin.3daymin         | shum.2m_min.diff              |                               | wspd.10m_min.6daymax           |
| hpbl_daymin.6daymin             | lts_nightmin.6daymin          |                               |                                |
| pres.sfc_min.diff               | mcdc_9x9_nightmax.3daymin     |                               |                                |
| apcp_daymin.3daymax             |                               |                               |                                |
| Selected via 50th Percentile QR |                               |                               |                                |
| Summer O <sub>3</sub>           | Summer PM <sub>2.5</sub>      | Winter O <sub>3</sub>         | Winter PM <sub>2.5</sub>       |
| rhum.2m_mean                    | air.2m_max                    | dsrwrf_mean                   | hpbl_mean                      |
| air.2m_max                      | air.sfc_9x9_nightmin.6daymax  | wspd.10m_mean                 | vwnddir.10m_mean               |
| dsrwrf_daymin.3daymean          | crain_9x9_nightmax            | dsrwrf_daymean.diff           | wspd.10m_daymax.3daymax        |
| vwnddir.10m_mean                | wspd.10m_max.3daymean         | vwnddir.10m_mean              | crain_9x9_nightmax             |
| crain_9x9_daymean               | vwnddir.10m_mean              | lts_daymin                    | wspd.10m_nightmax              |
| fire                            | lftx4_mean                    | shum.2m_min                   | rhum.2m_mean                   |
| tke.hl1_9x9_daymax              | lts_daymin                    | uwnddir.10m_mean              | uwnddir.10m_mean               |
| uwnddir.10m_daymean.3daymean    | uwnddir.10m_daymean.3daymean  | crain_9x9_daymax              | wspd.10m_max.3daymin           |
| air.sfc_9x9_daymin.3daymean     | shum.2m_daymean.diff          | dsrwrf_min.3daymin            | rpi_max                        |
| rpi_max                         | crain_9x9_max.6daymean        | fire                          | uwnddir.10m_nightmean.3daymean |
| lts_mean                        | rpi_max                       | air.sfc_9x9_mean.6daymean     | dsrwrf_daymin.6daymax          |
| dsrwrf_min.6daymin              | vwnd.500_min                  | hpbl_daymax                   | lftx4_nightmin.3daymean        |
| vwnd.500_min                    | vwnd.500_daymax.6daymax       | hcddc_9x9_daymax              | shum.2m_nightmin.6daymean      |
| hpbl_nightmean.3daymin          | pres.sfc_max                  | pres.sfc_nightmin.6daymean    | fire                           |
| vvel.hl1_mean.6daymean          | hgt.850_max.6daymax           | rpi_nightmax.6daymean         |                                |
| pres.sfc_mean.diff              |                               | air.sfc_9x9_nightmin.diff     |                                |
| rhum.2m_max.diff                |                               | lts_daymax.6daymin            |                                |
| vwnd.500_min.diff               |                               | mcdc_9x9_nightmax.3daymin     |                                |

Title Page

Abstract

Introduction

Conclusions

References

Tables

Figures

⏪

⏩

◀

▶

Back

Close

Full Screen / Esc

Printer-friendly Version

Interactive Discussion



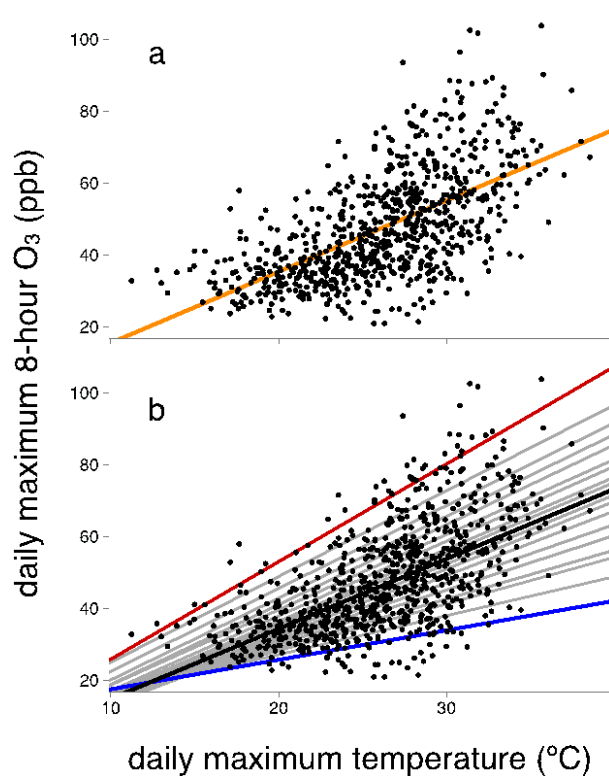


**Figure 1.** Daily maximum 8 h  $O_3$  vs. maximum daily temperature for example site in Essex County, MA. An ordinary least squares regression line (a) captures the general trend, but is unable to represent the increase of variability in the distribution with increasing temperature. Using individual quantile regressions ranging from 5th to 95th percentiles (b), the increased sensitivity of higher quantiles to increased temperatures becomes apparent.

Meteorological drivers of air quality extremes

W. C. Porter et al.

Title Page

Abstract

Introduction

Conclusions

References

Tables

Figures

◀

▶

◀

▶

Back

Close

Full Screen / Esc

Printer-friendly Version

Interactive Discussion



## Meteorological drivers of air quality extremes

W. C. Porter et al.

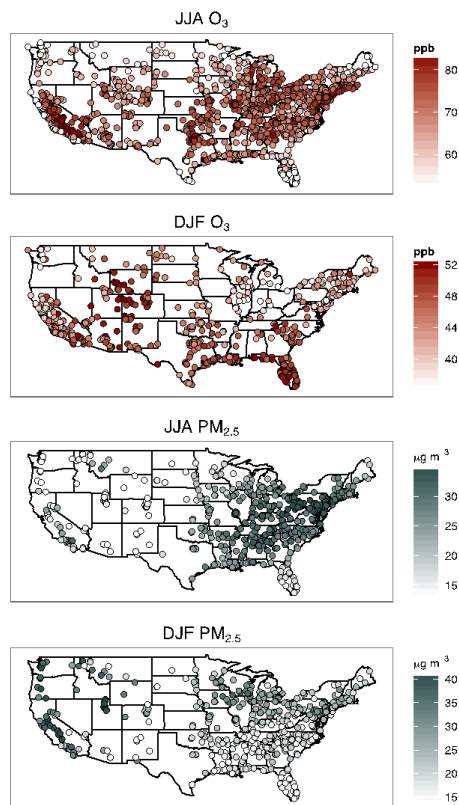


**Figure 2.** Location of AQS stations included in this study. The magnitude of each station's 95th percentile measurement is indicated by color.

[Title Page](#)[Abstract](#)[Introduction](#)[Conclusions](#)[References](#)[Tables](#)[Figures](#)[Back](#)[Close](#)[Full Screen / Esc](#)[Printer-friendly Version](#)[Interactive Discussion](#)

Meteorological drivers of air quality extremes

W. C. Porter et al.

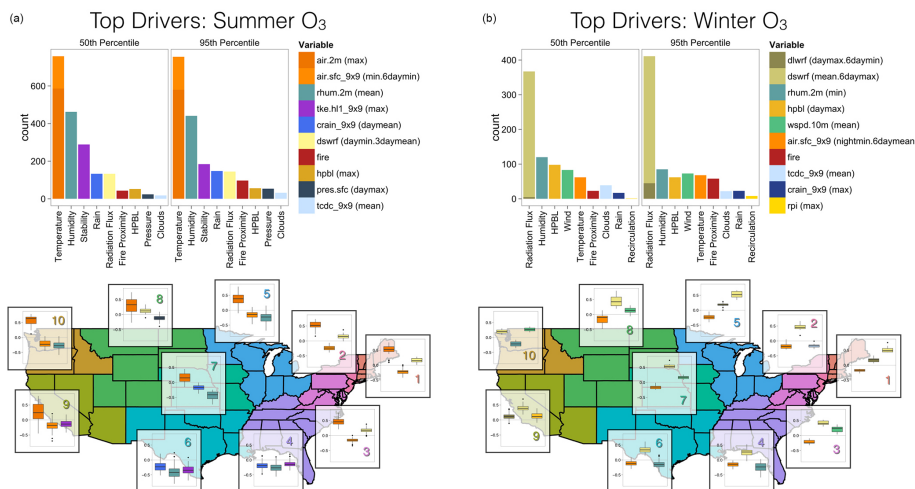


**Figure 3.** (a) Numbers of stations at which normalized 95th percentile QR coefficients for selected variables were in the top 2 out of all included variables (above) for summer  $O_3$ , and boxplots of normalized regression coefficients for top 3 drivers in each region (below). Colors on boxplots correspond to legend in above panel. EPA Region numbers are inset on top-right of boxplot panels. (b) Same as Fig. 3a, but for winter  $O_3$ .

Title Page

Abstract Introduction

Conclusions References

Tables Figures

◀ ▶

◀ ▶

Back Close

Full Screen / Esc

Printer-friendly Version

Interactive Discussion



Meteorological drivers of air quality extremes

W. C. Porter et al.

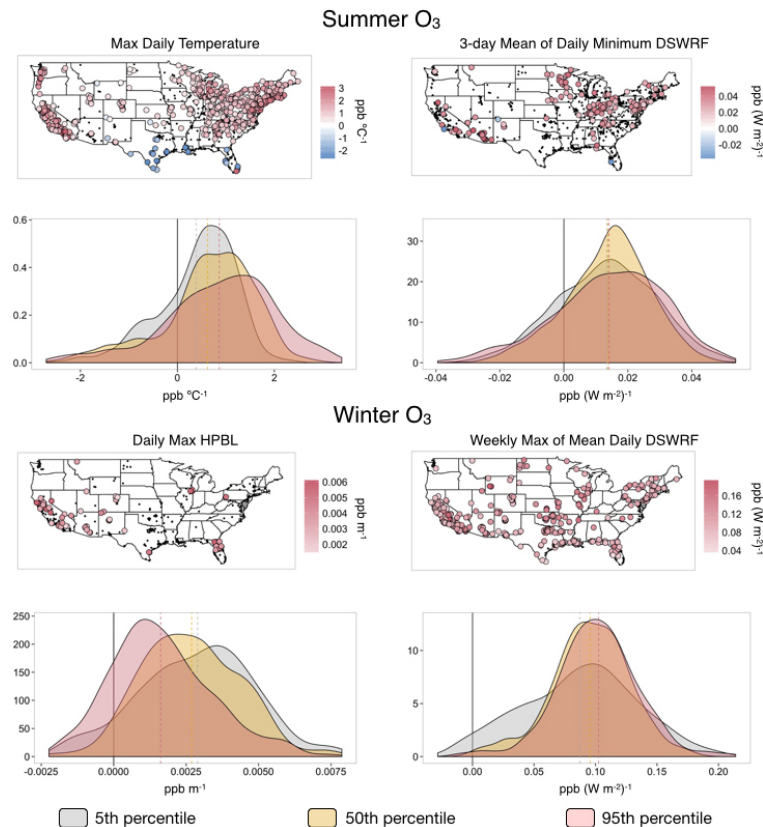


**Figure 4.** Spatial and frequency distributions for key drivers of summer (top) and winter (bottom) O<sub>3</sub>. Maps show 95th percentile O<sub>3</sub> sensitivities to selected meteorological variables at stations where that variable was most important (defined as being one of the top 2 normalized drivers). Below each map, histograms show the distribution of sensitivities for the 5th (blue), 50th (gray), and 95th (red) percentiles at all sites.

Title Page

Abstract Introduction

Conclusions References

Tables Figures

◀ ▶

◀ ▶

Back Close

Full Screen / Esc

Printer-friendly Version

Interactive Discussion



## Meteorological drivers of air quality extremes

W. C. Porter et al.

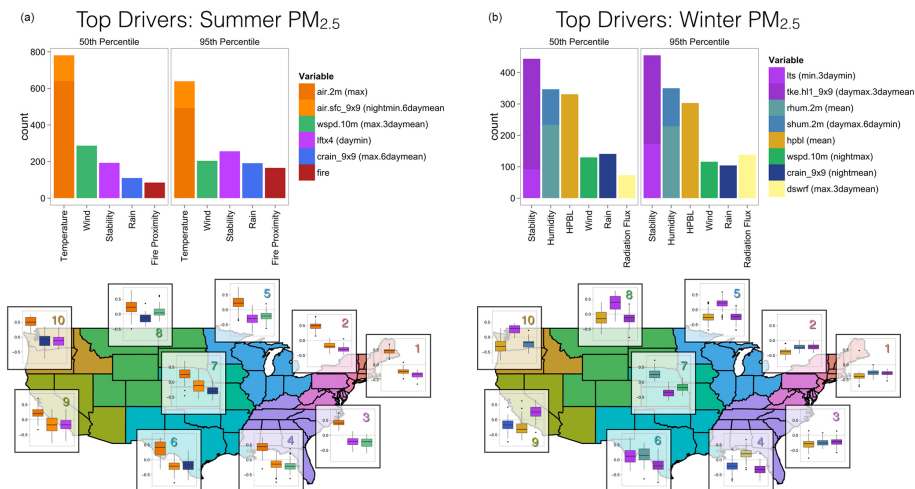


**Figure 5.** (a) Same as Fig. 3a but for summer PM<sub>2.5</sub>. (b) Same as for Fig. 3a but for winter PM<sub>2.5</sub>.

Title Page

Abstract

Introduction

Conclusions

References

Tables

Figures



Back

Close

Full Screen / Esc

Printer-friendly Version

Interactive Discussion



Meteorological drivers of air quality extremes

W. C. Porter et al.

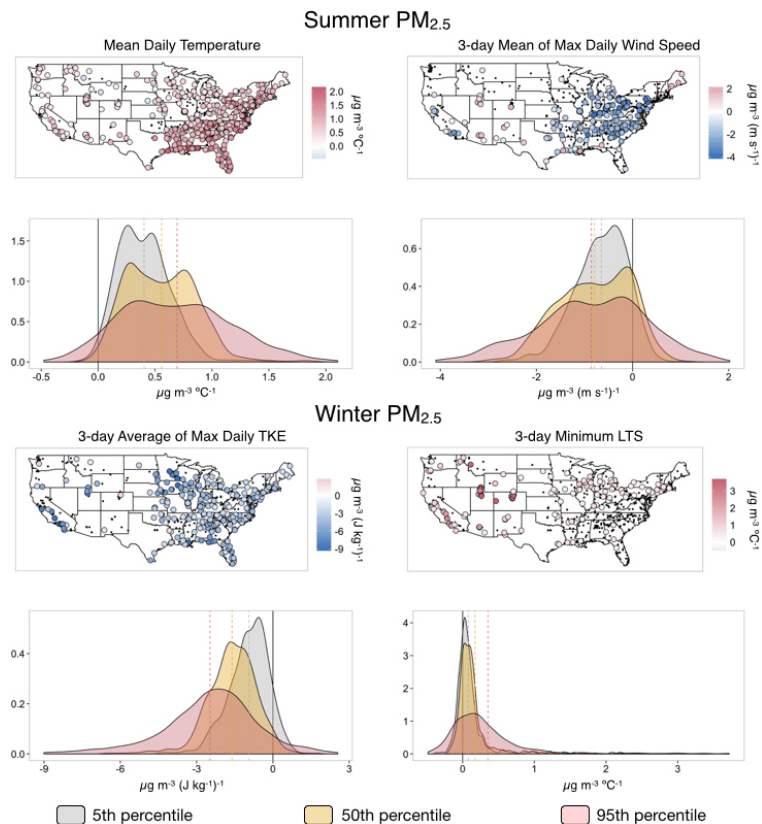


Figure 6. Same as Fig. 4 but for PM<sub>2.5</sub>.



Title Page

Abstract Introduction

Conclusions References

Tables Figures

◀ ▶

◀ ▶

Back Close

Full Screen / Esc

Printer-friendly Version

Interactive Discussion

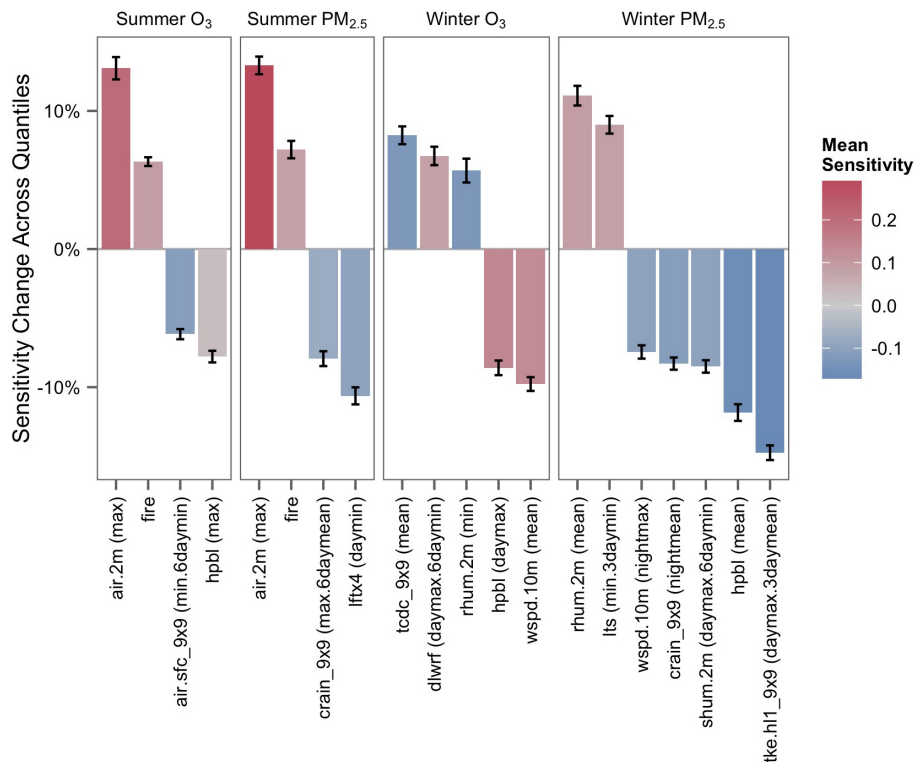


**Figure 7.** Estimate of how the pollutant concentrations sensitivity to meteorological driver varies with pollution level (0% = uniform sensitivity). Values shown here are the weighted least squares regressions performed on QR coefficients as a function of quantile for variable drivers with a mean sensitivity change of at least 5%, by species and season. Color of bars show mean normalized sensitivities (roughly equivalent to slopes expected from an ordinary least squares regression), while magnitudes of bars show mean percent change across quantiles, averaged over all stations. Error bars indicate standard error of the mean.

## Meteorological drivers of air quality extremes

W. C. Porter et al.

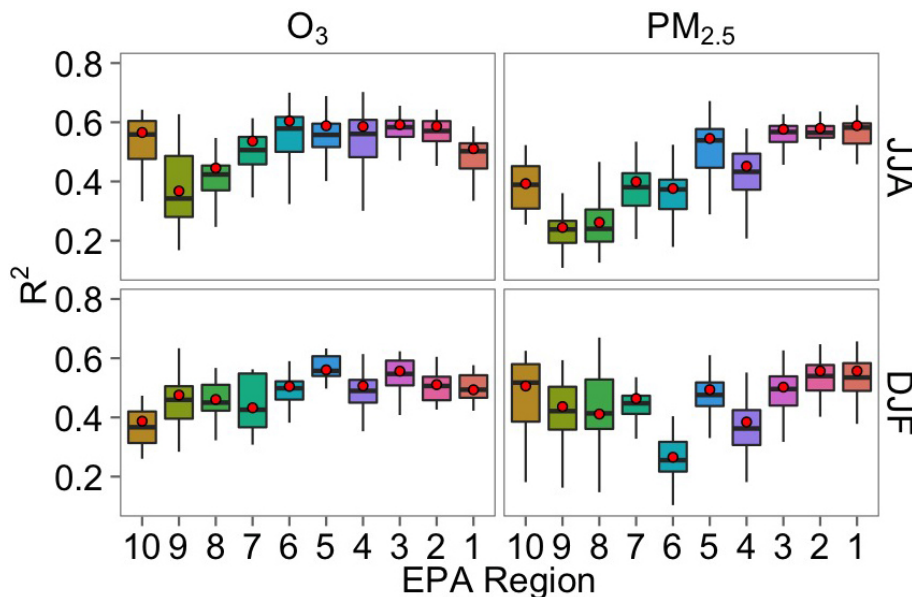


**Figure 8.** Ordinary least squares coefficient of determination ( $R^2$ ) between observed pollutant concentrations and the reduced set of meteorological variables selected in this analysis. Results are shown by pollutant ( $O_3$  or  $PM_{2.5}$ ), EPA region (see Figs. 3 and 5), and season (JJA = summer, DJF = winter). Red circles indicate median values using the full set of variables, for comparison. Refer to Table 2 for the listing of the reduced and full set of variables. Boxplot whiskers mark 5th and 95th percentile  $R^2$  values.

Title Page

Abstract

Introduction

Conclusions

References

Tables

Figures



Back

Close

Full Screen / Esc

Printer-friendly Version

Interactive Discussion

